Z. Phys. A 358, 407–413 (1997)

ZEITSCHRIFT
FÜR PHYSIK A

Diffractive phenomena and shadowing in deep-inelastic scattering

G. Piller, G. Niesler, W. Weise

Physik Department, Technische Universität München, D-85747 Garching, Germany

Received: 1 December 1996 / Revised version: 17 February 1997
Communicated by A. Schäfer

Abstract. Shadowing effects in deep-inelastic lepton-nucleus scattering probe the mass spectrum of diffractive leptoproduction from individual nucleons. We explore this relationship using current experimental information on both processes. In recent data from the NMC and E665 collaboration, taken at small $x \ll 0.1$ and $Q^2 \lesssim 1\,GeV^2$, shadowing is dominated by the diffractive excitation and coherent interaction of low mass vector mesons. If shadowing is explored at small $x \ll 0.1$ but large $Q^2 \gg 1\,GeV^2$ as discussed at HERA, the situation is different. Here dominant contributions come from the coherent interaction of diffractively produced heavy mass states. Furthermore we observe that the energy dependence of shadowing is directly related to the mass dependence of the diffractive production cross section for free nucleon targets.

PACS: 13.60.-r; 13.60.Le; 12.40.Vv

1 Introduction

In recent years diffractive photo- and leptoproduction of hadrons has become a field of growing interest. The diffractive excitation of heavy hadronic states with invariant masses $M_X \lesssim 5\,GeV$ has been investigated for photoproduction at FNAL [1]. Recent data from HERA explore the kinematic region $8\,GeV^2 < Q^2 < 100\,GeV^2$ and $M_X \lesssim 15\,GeV$ [2, 3, 4, 5, 6].

While diffractive photo- and leptoproduction of hadrons from nucleons is an interesting subject all by itself, it also plays a major role in the shadowing phenomena observed in high energy (virtual) photon-nucleus interactions. Shadowing in deep-inelastic lepton scattering is important at small values of the Bjorken scaling variable $x = Q^2/2M\nu$, where $q^\mu = (\nu, \boldsymbol{q})$ is the photon four-momentum in the lab frame with $Q^2 = -q^2$, and M stands for the nucleon mass. Here plenty of new data have become available from high precision experiments at FNAL (E665) [7, 8] and CERN (NMC) [9]. Because of the fixed target nature of these experiments the average available momentum transfer is small, $Q^2 \lesssim 1\,GeV^2$ at $x \ll 0.1$. Currently options to accelerate ions at HERA are under discussion. This would allow to investigate shadowing effects at $x \ll 0.1$ also at large $Q^2 \gg 1\,GeV^2$ [10].

In this paper we systematically explore nuclear shadowing in different kinematic regimes using the available experimental information on diffractive production processes from nucleons. Since the connection between diffraction and shadowing is most evident for processes involving a pair of target nucleons, we will focus on shadowing effects in deuterium. We find that in the kinematic regime of the E665 and NMC measurements shadowing is mainly due to the diffractive excitation and multiple scattering of vector mesons. This would be different at HERA, where the diffractive production of heavy mass states with $M_X^2 \sim Q^2$ would play a dominant role.

Nuclear shadowing in deep-inelastic scattering can also reveal details on diffractive processes from individual nucleons. For example, the energy dependence of nuclear shadowing is directly related to the dependence of the diffractive production cross section on M_X, the mass of the final hadronic state.

This paper is organized as follows: the available data on diffractive photo- and leptoproduction of hadrons are briefly summarized and discussed in Sec.2. In Sec.3 we review the relationship between shadowing and diffraction. The diffractive production cross sections from Sec.2 are then used to investigate shadowing for deuterium. Conclusions follow in Sec.4.

2 Diffractive production of hadrons from free nucleons

Consider the diffractive production of hadrons in the interaction of high energy real or virtual photons with free nucleons, $\gamma^* + N \to X + N$. As in diffractive hadron-hadron collisions such processes are important at small transfered momenta. The corresponding cross sections drop exponentially with $t = (p - p')^2 = k^2 \approx -\boldsymbol{k}^2$, where p and p' are the momenta of the initial and final nucleon. For our considerations we choose the laboratory frame where the target is at rest, $p^\mu = (M, \boldsymbol{0})$, and fix the z-axis to be parallel to the photon momentum: $q^\mu = (\nu, \boldsymbol{0}_\perp, \sqrt{Q^2 + \nu^2})$. The production of a hadronic final state X with an invariant mass M_X requires a minimal momentum transfer:

[1] Work supported in part by BMBF

$$k_{z,min} \simeq \frac{Q^2 + M_X^2}{2\nu} = Mx\left(1 + \frac{M_X^2}{Q^2}\right). \quad (1)$$

The diffractive excitation, with t required to be small, of heavy hadronic states is therefore possible only at sufficiently large photon energies ν or, equivalently, at small values of the Bjorken variable x.

In diffractive leptoproduction it is common to introduce the variable

$$x_{\mathbb{P}} = \frac{(p-p')\cdot q}{p\cdot q} = \frac{Q^2 + M_X^2 - t}{Q^2 + W^2 - M^2} \approx \frac{Q^2 + M_X^2}{Q^2 + W^2}, \quad (2)$$

with $W^2 = (p+q)^2 \approx 2M\nu - Q^2$. The notation $x_{\mathbb{P}}$ is a reminder of pomeron phenomenology. In terms of this variable,

$$k_{z,min} \approx Mx_{\mathbb{P}}. \quad (3)$$

Our aim here is to investigate the relation between diffractive (virtual) photoproduction of hadrons from nucleons and shadowing corrections in deep-inelastic lepton-nucleus scattering. For this purpose we need to consider the forward diffractive production cross section with $t \approx t_{min} = -k_{z,min}^2 \approx 0$. We split it into the production cross section for low mass vector mesons ρ, ω and ϕ, and the cross section for hadronic final states carrying larger invariant masses $M_X^2 > 1\,GeV^2$:

$$\left.\frac{d\sigma^D_{\gamma^* N}}{dM_X^2 dt}\right|_{t\approx 0} = \sum_{V=\rho,\omega,\phi} \left.\frac{d\sigma^V_{\gamma^* N}}{dM_X^2 dt}\right|_{t\approx 0} + \left.\frac{d\sigma^{cont}_{\gamma^* N}}{dM_X^2 dt}\right|_{t\approx 0}. \quad (4)$$

First we explore this cross section in the kinematic domain of nuclear shadowing as measured by the E665 and NMC experiments. In this region at $x \ll 0.1$ the experimentally accessible values for the momentum transfer Q^2 are small. As an example, one has for $x < 0.005$ an average momentum transfer $\overline{Q^2} < 1\,GeV^2$ [7, 8, 9]. For a qualitative discussion, it is therefore useful first to consider diffractive (real) photoproduction processes for which more experimental data are available than in leptoproduction at finite Q^2.

2.1 Photoproduction

In the case of photoproduction the vector meson contribution to the diffractive cross section in (4) can be described within the framework of generalized vector meson dominance [11, 12]. One finds:

$$\left.\frac{d\sigma^V_{\gamma N}}{dM_X^2 dt}\right|_{t\approx 0} = \frac{e^2}{16\pi}\frac{\Pi^V(M_X^2)}{M_X^2}\sigma_{VN}^2, \quad (5)$$

where

$$\Pi(M_X^2) = \frac{1}{12\pi^2}\frac{\sigma(e^+e^- \to hadrons)}{\sigma(e^+e^- \to \mu^+\mu^-)} \quad (6)$$

is the photon spectral function as measured in e^+e^- annihilation and $e^2/4\pi = 1/137$. The contribution of the narrow ω- and ϕ-mesons to the photon spectral function is given by:

$$\Pi^V(M_X^2) = \left(\frac{m_V}{g_V}\right)^2 \delta(M_X^2 - m_V^2), \quad (7)$$

for $V = \omega, \phi$, with the couplings $g_\omega = 17.0$, $g_\phi = 12.9$ and masses $m_\omega = 782\,MeV$, $m_\phi = 1019\,MeV$ [11]. A comparison of (5) with recent photoproduction data taken at HERA gives for the ω–nucleon and ϕ–nucleon cross sections at an average center of mass energy $\overline{W} = 80\,GeV$ and $\overline{W} = 70\,GeV$, respectively:

$$\sigma_{\omega N} = 26.0 \pm 2.5\,mb\,[13] \quad \text{and} \quad \sigma_{\phi N} = 19 \pm 7\,mb\,[14]. \quad (8)$$

These values are in agreement with an analysis of nuclear effects in ω- and ϕ-production [11] in the framework of vector meson dominance. Unlike the ω- and ϕ-meson the ρ-meson has a large width from its strong coupling to two-pion states. Therefore neither should the ρ-meson contribution to the photon spectral function be approximated by a δ-function, nor is it useful to separate contributions from resonant and non-resonant two-pion pairs. Both are accounted for in the $\pi^+\pi^-$ part of the photon spectral function which is given by the pion form factor F_π:

$$\Pi^\rho(M_X^2) = \frac{1}{48\pi^2}\Theta(M_X^2 - 4m_\pi^2) \times \times \left(1 - \frac{4m_\pi^2}{M_X^2}\right)^{3/2} \left|F_\pi\left(M_X^2\right)\right|^2, \quad (9)$$

where m_π and $M_X = M_{\pi\pi}$ are the invariant masses of the pion and the $\pi^+\pi^-$ pairs. With an effective $\pi^+\pi^-$–nucleon cross section $\sigma_{\pi\pi N} = 30\,mb$ the main features of the mass distribution $d\sigma^{\pi\pi}_{\gamma N}/dM_{\pi\pi}$ for $M_{\pi\pi} < 1\,GeV$, as measured recently by the ZEUS collaboration [15], are reproduced. Figure 1 shows our calculated mass spectrum of $\pi^+\pi^-$ pairs using (5,9) in comparison with recent data from ZEUS [15]. A perfect fit is obtained when small corrections from a possible mass dependence of $\sigma_{\pi\pi N}$ are included (for details see [12]). For the pion form factor we have used the improved vector meson dominance form from [16] which reproduces the measured F_π very well.

We note that the observed energy dependence of diffractive vector meson production is consistent with Regge phenomenology:

$$\left.\frac{d\sigma^V_{\gamma N}}{dt}\right|_{t\approx 0} \approx W^{4(\alpha_{\mathbb{P}}(0)-1)} = W^{4\epsilon}, \quad (10)$$

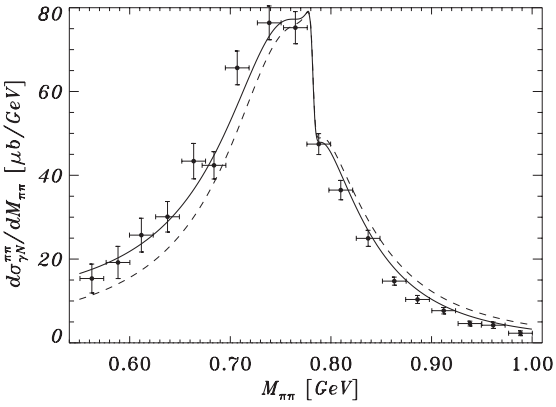

Fig. 1. The mass distribution $d\sigma^{\pi\pi}_{\gamma N}/dM_{\pi\pi}$ of diffractive photoproduction in the rho meson region. The *dashed curve* shows the contribution from the $\pi^+\pi^-$ part of the photon spectral function (9). The *full curve* includes a small mass dependence of $\sigma_{\pi\pi N}$ [12]. The data are taken from the ZEUS collaboration [15]

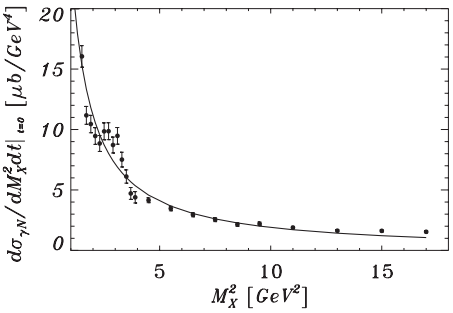

Fig. 2. The diffractive photoproduction cross section for large masses M_X. The *full curve* shows the fit from (12). The data are taken from [1] and extrapolated to $t = 0$ using an average slope $b = 5\,GeV^{-2}$

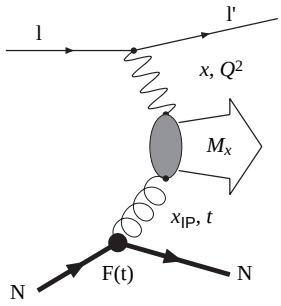

Fig. 3. Regge picture of diffractive lepton-nucleon scattering [19]

where $\alpha_{I\!P}(t = 0) = 1 + \epsilon \approx 1.1$ is the soft pomeron intercept (see e.g. [17]). This translates into an energy dependence of the effective vector meson-nucleon cross section:

$$\sigma_{VN} \sim W^{2(\alpha_{I\!P}(0)-1)} = W^{2\epsilon} \approx W^{0.2}. \tag{11}$$

The second term in (4) describes the $\sim 1/M_X^2$ behaviour of the diffractive production cross section for large masses M_X. Guided by Regge phenomenology [18] we use the parametrization:

$$\left.\frac{d\sigma_{\gamma N}^{cont}}{dM_X^2 dt}\right|_{t\approx 0} = C\frac{W^{4\epsilon}}{M_X^{2(1+\epsilon)}}. \tag{12}$$

With $C = 8.2\,\mu b/GeV^{2(1+\epsilon)}$ we obtain a fair description of the measured diffractive cross section from [1] for $M_X > 1.5\,GeV$ as shown in Fig.2.

2.2 Leptoproduction

Diffractive leptoproduction data have recently become available at large Q^2 ($8\,GeV^2 < Q^2 < 100\,GeV^2$) from the H1 [2, 3] and ZEUS [4, 5, 6] collaborations at HERA. The corresponding diffractive production cross section is usually expressed in terms of the diffractive structure function $F_2^{D(4)}$. At small values $x < 0.1$ of the Bjorken variable we have:

$$F_2^{D(4)}(x, Q^2; x_{I\!P}, t) = \frac{Q^2}{\pi e^2}\frac{d^2\sigma^D_{\gamma^* N}}{dx_{I\!P}dt}. \tag{13}$$

Up to now no accurate data on the t-dependence of $F_2^{D(4)}$ are available. Data exist only for the t-integrated structure function

$$F_2^{D(3)}(x, Q^2; x_{I\!P}) = \int_{-\infty}^{0} dt\, F_2^{D(4)}(x, Q^2; x_{I\!P}, t). \tag{14}$$

In the kinematic region of current HERA experiments one finds that $F_2^{D(3)}$ can be factorized as follows:

$$F_2^{D(3)}(x, Q^2; x_{I\!P}) = \frac{A(\beta, Q^2)}{x_{I\!P}^{n(\beta)}}, \tag{15}$$

with $\beta = x/x_{I\!P}$. Although first data on $F_2^{D(3)}$ were consistent with a constant n [2, 4, 5], most recent measurements from H1 indicate a weak β-dependence of n [3].

For the investigation of nuclear shadowing we need the diffractive production cross section at $t \approx 0$, or equivalently $F_2^{D(4)}(x, Q^2; x_{I\!P}, t \approx 0)$, in a suitably parametrized form. We are guided again by Regge phenomenology and the picture, Fig. 3, which suggests the following ansatz for $F_2^{D(4)}$ [19]:

$$F_2^{D(4)}(x, Q^2; x_{I\!P}, t) = \frac{D(\beta, Q^2)}{x_{I\!P}^{2\alpha(\beta,t)-1}}F^2(t). \tag{16}$$

Here we have introduced the isoscalar nucleon form factor $F(t)$, as in high energy hadron-nucleon scattering [20]. At small t we use:

$$F(t) = e^{bt/2}, \tag{17}$$

with $b \approx 4.6\,GeV^{-2}$. We expand

$$\alpha(\beta, t) \approx \alpha_0(\beta) + \alpha_1(\beta)\,t + \ldots \tag{18}$$

For example, if α represents a soft pomeron we expect $\alpha_0 = \alpha_{I\!P}(t = 0) \approx 1.1$, and conventional Regge behavior corresponds to $\alpha_1 = 0.25\,GeV^{-2}$. The remaining function $D(\beta, Q^2)$ needs to be determined by comparison with the available data on $F_2^{D(3)}$. We find:

$$\begin{aligned} F_2^{D(4)}(x, Q^2; x_{I\!P}, t = 0) &= \frac{D(\beta, Q^2)}{x_{I\!P}^{2\alpha_0-1}}, \\ &= (b - 2\alpha_1 \ln x_{I\!P})\, F_2^{D(3)}(x, Q^2; x_{I\!P}). \end{aligned} \tag{19}$$

Omitting a possible logarithmic Q^2-dependence of the measured $F_2^{D(3)}$ we employ the parametrization [4]:

$$A(\beta, Q^2) = d\left[\beta(1-\beta) + \frac{f}{2}(1-\beta)^2\right] \tag{20}$$

in (15). We then use the following (different) sets of parametrizations motivated by the H1 and ZEUS data, respectively:

(i) We use $n = 1.19$ as found by the H1 collaboration [2]. Together with the conventional Regge value $0.25\,GeV^{-2}$ for α_1 we take $d = 0.03$ and $f = 0.6$. The resulting $\alpha_0 \approx 1.13$ is close to the intercept $\alpha_{I\!P}(0) \approx 1.1$ expected for a soft pomeron.

(ii) The ZEUS collaboration recently found $n = 1.46$ [5], which seems to be incompatible with the simple soft pomeron exchange picture[1]. In this case we choose $\alpha_1 = 0$, $d = 0.007$ and $f = 0.6$. Here we get $\alpha_0 = (n+1)/2 = 1.23$. Note that a "hard" pomeron intercept $\alpha_0 \approx 1.5$ would lead to $n \approx 2$ which is too large.

[1] In previous [4] and most recent [6] ZEUS data $n \approx 1.3$ was found. A reanalysis of the data is in progress [35]

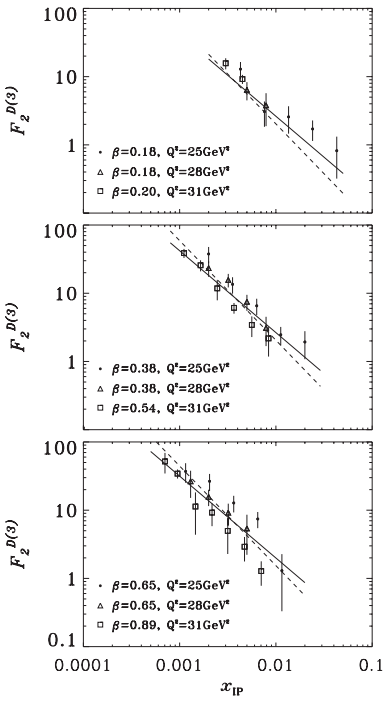

Fig. 4. The diffractive structure function $F_2^{D(3)}$ as a function of $x_{\mathbf{P}}$. The *full* and *dashed curves* correspond to the parametrizations (i) and (ii) in Sect. 2.2. The data are taken from H1 (*dotted*) [2] and ZEUS (*triangles*) [4], (*squares*) [5]

In Fig. 4 we compare our parametrizations to the $x_{\mathbf{P}}$-dependence of the measured structure function $F_2^{D(3)}$ as found by the H1 and ZEUS experiments. Note that a small fraction of the data includes diffractive dissociation of the nucleon target. In the present analysis we have not corrected for these events. Furthermore we observe that the t-dependence, $F_2^{D(4)} \sim e^{Bt}$, of the diffractive structure function is determined by the slope

$$B(x_{\mathbf{P}}) = b - 2\alpha_1 \ln x_{\mathbf{P}}. \tag{21}$$

In the kinematic range $10^{-4} < x_{\mathbf{P}} < 0.05$ of HERA we find $B \approx$ (6–9) GeV^{-2} for the H1 set (i) and $B \approx 5\,GeV^{-2}$ for the ZEUS set (ii).

3 Shadowing effects in deep-inelastic scattering from deuterium

The connection between diffractive (virtual) photoproduction and nuclear shadowing can be established most clearly for double scattering contributions to nuclear deep-inelastic scattering, i.e. processes in which the incoming photon beam interacts with two nucleons inside the target[2]. To avoid complications from higher order multiple scattering we investigate shadowing effects for deuterium. This will be done in the laboratory frame. Realistic nuclear wave functions are established only in this frame.

The photon-deuteron forward scattering amplitude can be written as the sum of single and double scattering contributions:

$$\mathcal{A}_{\gamma^* d} = \mathcal{A}^{(1)}_{\gamma^* p} + \mathcal{A}^{(1)}_{\gamma^* n} + \mathcal{A}^{(2)}_{\gamma^* d}. \tag{22}$$

[2] A similar analysis for hadron-nucleus collisions can be found in [21]

The $\mathcal{A}^{(1)}$ amplitudes describe the incoherent scattering of the (virtual) photon from the proton or neutron, while $\mathcal{A}^{(2)}$ accounts for the coherent interaction of the projectile with both nucleons. At large photon energies $\nu > 3\,GeV$, or small values of $x < 0.1$ respectively, the double scattering amplitude is dominated by diffractive excitations of the photon to hadronic intermediate states. We restrict ourselves to the dominant diffractive photoproduction in the forward direction described by the amplitude $T_{\gamma^* N \to XN}$. Treating the deuteron target in the non-relativistic limit gives [22]:

$$\mathcal{A}^{(2)}_{\gamma^* d} = -\frac{1}{\pi M} \int_{-\infty}^{\infty} dz |\psi_d(\mathbf{0}_\perp, z)|^2 \sum_X \int_{-\infty}^{\infty} dk_z \times$$
$$\times\, T_{\gamma^* N \to XN} \frac{e^{ik_z z}}{\nu^2 - (q_z + k_z)^2 - M_X^2 + i\epsilon} T_{XN \to \gamma^* N}. \tag{23}$$

Here $\psi_d(\boldsymbol{r})$ is the deuteron wave function with the normalization $\int d\boldsymbol{r} |\psi_d(\boldsymbol{r})|^2 = 1$. We sum over all diffractively excited hadronic states X with invariant mass M_X and four-momentum $(\nu, \mathbf{0}_\perp, q_z + k_z)$. After integrating over the longitudinal momentum transfer k_z the double scattering contribution to the total photon-deuteron cross section reads:

$$\delta\sigma_{\gamma^* d} = \frac{Im\mathcal{A}^{(2)}_{\gamma^* d}}{4M\nu} = -16\pi \int_{4m_\pi^2}^{W^2} dM_X^2 \left.\frac{d^2\sigma^D_{\gamma^* N}}{dM_X^2 dt}\right|_{t\approx 0}$$
$$\times \int_0^\infty dz\, |\psi_d(\mathbf{0}_\perp, z)|^2$$
$$\times \left[\left(1 - 2\left(\frac{Re\,T}{Im\,T}\right)^2\right)\cos(z/\lambda) - 2\frac{Re\,T}{Im\,T}\sin(z/\lambda)\right]. \tag{24}$$

Here $T \equiv T_{\gamma^* N \to XN}$, and $d^2\sigma^D_{\gamma^* N}/dM_X^2 dt|_{t\approx 0}$ is the forward diffractive cross section for the production of hadrons with invariant mass M_X:

$$\sum_X \left.\frac{|T_{\gamma^* N \to XN}|^2}{(2M\nu)^2}\right|_{t\approx 0} = 16\pi \int_{4m_\pi^2}^{W^2} dM_X^2 \left.\frac{d^2\sigma^D_{\gamma^* N}}{dM_X^2 dt}\right|_{t\approx 0}. \tag{25}$$

In eq.(24) we sum over all diffractive excitations which are kinematically permitted, i.e. $4m_\pi^2 \le M_X^2 \le W^2$. The longitudinal propagation length λ of the intermediate hadronic state X is the inverse of the minimal momentum transfer (1) necessary for its diffractive excitation:

$$\lambda = \frac{1}{k_{z,min}} = \frac{2\nu}{Q^2 + M_X^2}. \tag{26}$$

Neglecting the real part of the diffractive production amplitudes leads to the well known result [23]:

$$\delta\sigma_{\gamma^* d} = -8\pi \int_{4m_\pi^2}^{W^2} dM_X^2 \left.\frac{d^2\sigma^D_{\gamma^* N}}{dM_X^2 dt}\right|_{t\approx 0} \mathcal{F}_d(\lambda^{-1}), \tag{27}$$

with the longitudinal deuteron form factor

$$\mathcal{F}_d(\lambda^{-1}) = \int_{-\infty}^{\infty} dz |\psi_d(\mathbf{0}_\perp, z)|^2 \cos(z/\lambda). \tag{28}$$

As soon as the longitudinal propagation length $\lambda(M_X^2)$ of a certain hadronic intermediate state exceeds the average nucleon-nucleon distance in the nuclear target, it will contribute to double scattering and therefore to shadowing. Since λ decreases with M_X, low mass diffractive excitations are important for

the onset of shadowing. If the propagation length of a specific hadronic intermediate state exceeds the target diameter, $\lambda > \langle r^2\rangle^{1/2} \sim 4\,fm$ for the deuteron, double scattering is not restricted since $\mathcal{F}_d \approx constant$. Therefore in a first approximation hadronic states with an invariant mass

$$M_X^2 < M_{max}^2 = \frac{W^2 + Q^2}{M\langle r^2\rangle^{1/2}} - Q^2 \tag{29}$$

contribute to double scattering. Combining eqs.(4,27,29) yields the following approximate equation for the shadowing correction:

$$\begin{aligned}\delta\sigma_{\gamma^* d} \approx & -8\pi\mathcal{F}_d(\lambda^{-1}\to 0) \\ & \left\{\int_{4m_\pi^2}^{M_0^2} dM_X^2 \sum_{V=\rho,\omega,\phi} \left.\frac{d\sigma^V_{\gamma^* N}}{dM_X^2 dt}\right|_{t\approx 0} + \right. \\ & \left. + \int_{M_0^2}^{M_{max}^2} dM_X^2 \left.\frac{d\sigma^{cont}_{\gamma^* N}}{dM_X^2 dt}\right|_{t\approx 0}\right\}, \\ = & -8\pi\mathcal{F}_d(0)\left\{\sum_V b_V\,\sigma(\gamma^* N\to VN) + \right. \\ & \left. + \overline{b_X}\,\sigma(\gamma^* N\to XN)\right\}, \end{aligned} \tag{30}$$

where $M_0 \sim m_\phi$. Here we have assumed an exponential t-dependence, e^{bt}, for the diffractive production cross sections. The corresponding slopes for vector meson production are denoted by b_V, while $\overline{b_X}$ stands for the average slope for the production of hadronic states X with $M_0^2 < M_X^2 < M_{max}^2$.

Using the parametrizations for the diffractive cross sections as derived in Sect. 2, we can now discuss shadowing in the deuteron for real and virtual photon beams.

3.1 Shadowing for real photons

It is instructive to apply (30) to real photon-deuteron scattering. The relevant diffractive scattering cross sections for this case are given by (5,12). We find:

$$\begin{aligned}\delta\sigma_{\gamma d} \approx & -8\pi\mathcal{F}_d(0)\left\{\sum_V b_V\,\sigma(\gamma N\to VN) + W^{4\epsilon}\frac{C}{\epsilon}\times\right. \\ & \left.\times\left[\frac{1}{M_0^{2\epsilon}} - \left(\frac{M\langle r^2\rangle^{1/2}}{W^2}\right)^{\epsilon}\right]\right\}. \end{aligned} \tag{31}$$

We observe two sources for the energy dependence of the shadowing correction $\delta\sigma_{\gamma d}$. First, the rising diffractive photoproduction cross sections $\sigma(\gamma N\to XN)\sim W^{4\epsilon}$ with $\epsilon\sim 0.1$ translate into a contribution to shadowing with a similar energy dependence. However this is not the only source for an increase of $\delta\sigma_{\gamma d}$ with W. With rising center of mass energy the propagation length λ also increases and allows for additional contributions to shadowing from diffractively produced states of large mass as can be seen from (29).

In Fig. 5 we show the shadowing correction $\delta\sigma_{\gamma d}$ calculated from (27). Here a realistic deuteron form factor (28) as obtained from the Paris potential [24] was used. For $\nu > 50\,GeV$ we find good agreement with the approximation in (31). The vector meson contribution to shadowing is proportional to $\nu^{2\epsilon}\approx\nu^{0.2}$ and dominates $\delta\sigma_{\gamma N}$ for $\nu < 300\,GeV$.

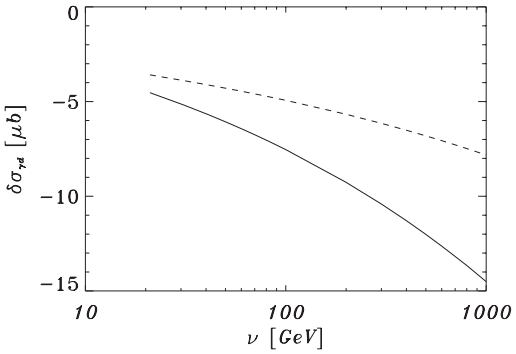

Fig. 5. The energy-dependence of the shadowing correction $\delta\sigma_{\gamma d}$ calculated from (27). The *dashed line* shows the vector meson contribution

At higher energies contributions from hadronic states of large mass also become important. In the energy range of present fixed target experiments, $\nu < 400\,GeV$, their increase with ν is stronger than $\nu^{0.2}$ due to the additional contributions from large mass states.

As already mentioned, recent data on nuclear shadowing from the E665 and NMC collaborations were taken at small momentum transfers $\overline{Q^2} \lesssim 1\,GeV^2$ for $x \ll 0.1$. The energy transfer in these experiments is typically $40\,GeV < \nu < 380\,GeV$ [7, 8, 9]. Therefore the conclusion just drawn applies here too: nuclear shadowing as measured by E665 and NMC is dominated by the diffractive excitation and multiple scattering of vector mesons. This observation is in agreement with a number of model calculations (see e.g. [25, 26, 27]). Nevertheless large mass states play their role even in the kinematic region of the E665 and NMC measurements as they are responsible for the leading twist nature of nuclear shadowing (see e.g. [27, 28, 29] and references therein).

In Fig. 6 we show the ratio of the total photon-deuteron cross section compared to twice the free photon-nucleon cross section, $R = \sigma_{\gamma d}/2\sigma_{\gamma N}$. For the free photon-nucleon cross section we use the empirical photon-proton cross section from [30] with the energy dependence $\sigma_{\gamma N}\sim W^{2\epsilon}\approx W^{0.2}$. Then the shadowing correction grows as $\delta\sigma_{\gamma d}/2\sigma_{\gamma d} = R - 1 \sim \nu^\epsilon \approx \nu^{0.1}$. We find that our results are well within the range

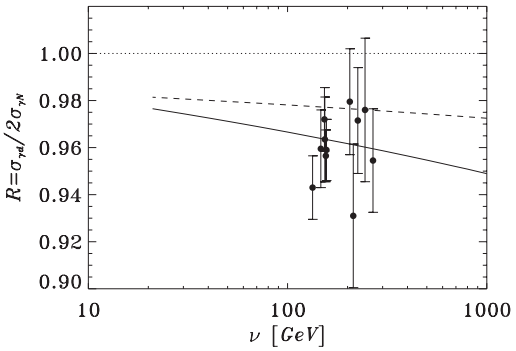

Fig. 6. The shadowing ratio $R = \sigma_{\gamma d}/2\sigma_{\gamma N}$ as a function of the photon energy. The *dashed line* shows the vector meson contribution. The experimental data are taken from the E665 collaboration [7]. (The energy values of the data have to be understood as average values which correspond to different x-bins.)

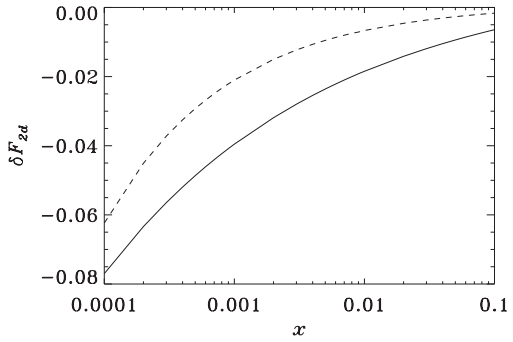

Fig. 7. The shadowing correction δF_{2d} from (27) at large $\overline{Q^2} \sim 25\,GeV^2$ plotted against x. For the diffractive structure function $F_2^{D(4)}$ we have used the parametrizations (i) (*full*) and (ii) (*dashed*) from Sect. 2.2

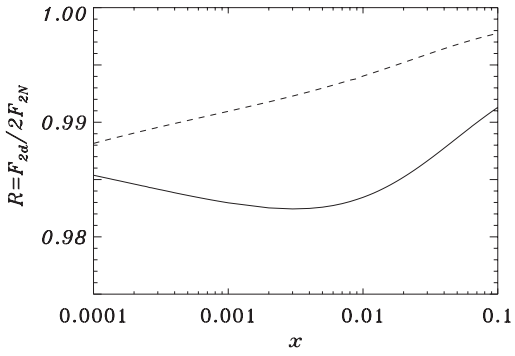

Fig. 8. The shadowing ratio $R = F_{2d}/2F_{2N}$ at large $\overline{Q^2} \sim 25\,GeV^2$. The *full* and *dashed curve* correspond to the diffractive structure function (i) and (ii) from Sect. 2.2, respectively. The nucleon structure function has been taken from [32] at $Q^2 = 25\,GeV^2$

of recent lepton-deuteron scattering data from the E665 collaboration [7] measured at $\overline{Q^2} \lesssim 0.5\,GeV^2$.

3.2 Shadowing at large Q^2

When expressed in terms of the diffractive structure function the double scattering contribution to the deuteron structure function, $\delta F_{2d} = \frac{Q^2}{\pi e^2}\,\delta\sigma_{\gamma^* d}$, becomes (30):

$$\delta F_{2d}(x,Q^2) \approx -8\pi\mathcal{F}_d(0)\int_{x_0}^{x_m} dx_{I\!P}\ \times \\ \times\, F_2^{D(4)}(x,Q^2;x_{I\!P},t\approx 0), \qquad (32)$$

where $x_m \approx 1/M\langle r^2\rangle^{1/2}$ and $x_0 \approx Q^2/W^2 \approx x$ for $x \ll 0.1$. An investigation of δF_{2d} using the parametrizations for $F_2^{D(4)}$ as derived in Sect. 2.2 yields, that shadowing is dominated at $x \ll 0.01$ by the leading contribution to the diffractive structure function in the limit of small $x_{I\!P} \ll 0.01$. Using (19) we obtain at small $x \ll 0.1$:

$$\delta F_{2d}(x,Q^2) \approx -8\pi\mathcal{F}_d(0)\,\frac{1}{x^{n-1}}\frac{d}{n}\ \times \\ \times\left\{(b-2\alpha_1\,\ln\,x)\,\frac{f+n-1}{n^2-1}\ - \right. \\ \left. -\ 2\alpha_1\frac{(1-f)(1-3n^2)+2n^3}{n(n^2-1)^2}\right\}. \qquad (33)$$

For the different parametrizations of the diffractive structure function $F_2^{D(4)}$ in Sect. 2.2 we find from (33) that at $x \ll 0.01$ shadowing increases with decreasing x as $\delta F_{2d} \sim x^{-0.25}$ for the parameter set (i), and $\delta F_{2d} \sim x^{-0.46}$ for (ii). This observation is confirmed by an explicit calculation of the double scattering correction using (27) together with the deuteron form factor as obtained from the Paris potential. The result for δF_{2d} is shown in Fig. 7. For $x < 0.01$ it agrees well with the approximation in (33). We conclude that at large $Q^2 \gtrsim 10\,GeV^2$ and small $x < 0.01$ shadowing is controlled by the behavior of the diffractive structure function at small values of $x_{I\!P}$, or equivalently at large hadronic masses M_X.

Recent data from HERA show that at corresponding values of $x \ll 0.01$ and $Q^2 \gtrsim 10\,GeV^2$ the inclusive nucleon structure function rises as $F_{2N} \sim x^{-\lambda}$ with $\lambda = 0.25 - 0.3$ [31]. Therefore we find that in this kinematic region $R = F_{2d}/2F_{2N}$ increases moderately with decreasing x for the parameter set (i) which is guided by the H1 data on the diffractive structure function. For the parameter set (ii) motivated by data from ZEUS we observe a slow decrease of the shadowing ratio with decreasing x. In Fig. 8 we present the results for the structure function ratio R using the free nucleon structure function from [32] taken at $Q^2 = 25\,GeV^2$.

A comparison with the results from the previous section demonstrates the qualitative difference between the energy dependence of shadowing at small and large Q^2.

A similar prediction was made recently by Kopeliovich and Povh [33]. They express the virtual photon-nucleon cross section at small x through the interaction of hadronic fluctuations of the virtual photon with different transverse sizes. The contribution of a certain hadronic fluctuation is given by its weight in the photon wave function, times its interaction cross section. The probability to find large size ($\sim 1/\Lambda_{QCD}$) quark-gluon configurations in the virtual photon is suppressed by Λ^2_{QCD}/Q^2, as compared to small configurations with transverse sizes $b^2 \sim Q^{-2}$. However since the interaction cross sections of such hadronic fluctuations are proportional to their transverse size, both give leading contributions $\sim 1/Q^2$ to the photon-nucleon cross section. This is different for the coherent interaction of the virtual photon with several nucleons as, in deep-inelastic scattering from nuclei at small x. For example the contribution of a hadronic fluctuation to double scattering is given by its weight in the photon wave function, multiplied by the *square* of its interaction cross section. Consequently large size configurations yield a leading $1/Q^2$–contribution to the double scattering cross section, while contributions from small size configurations are proportional to $1/Q^4$ and suppressed. Therefore multiple scattering contributions to the virtual photon-nucleus cross section at small x are dominated by the interaction of large-size hadronic fluctuations. The energy dependence of the interaction cross section of photon-induced large size quark-gluon configurations should be similar to the one observed in high energy hadron-hadron collisions, and therefore much weaker than the strong energy dependence of the nucleon structure function at small x and large Q^2.

Finally we emphasize that in contrast to the $Q^2 \sim 0$ case discussed in Sect. 3.1, the diffractive excitation of vector mesons is not relevant at large $Q^2 \gtrsim 10\,GeV^2$. This is simply a consequence of the strong decrease of vector meson produc-

tion cross sections with Q^2, e.g. $\sigma(\gamma^* N \to \rho N) \sim Q^{-\beta}$ with $\beta \approx 4.2$–5.0 [34]. From (30) we estimate the vector meson contribution to the shadowing correction δF_{2d} to be less than 3% at large Q^2.

4 Summary

Shadowing effects in deep-inelastic lepton-nucleus scattering are dominated by the diffractive excitation and coherent interaction of hadronic Fock states present in the wave function of the exchanged virtual photon. Therefore shadowing is closely related to diffractive leptoproduction of hadrons from individual nucleons. We have investigated this connection using the currently available experimental information for both processes. We find that in the kinematic regime of small $x \ll 0.1$ and small $Q^2 < 1\,GeV^2$, as in recent experiments from the NMC and E665 collaboration, shadowing is dominated by vector mesons. At large values of Q^2 the situation is different. Using data on the diffractive nucleon structure function from HERA we have shown that heavy mass states play a dominant role in shadowing at small $x \ll 0.1$ and large $Q^2 \gg 1\,GeV^2$. Furthermore we have demonstrated that the energy dependence of shadowing is directly related to the dependence of the diffractive production cross section on the mass of the final hadronic state. In view of these results, it appears that the currently discussed option of accelerating ions at HERA could add interesting new information about diffractive processes for nuclear and nucleon targets.

References

1. T.J. Chapin et al., Phys. Rev. **D 31** (1985) 17
2. H1 Collab., T. Ahmed et al., Phys. Lett. **B 348** (1995) 681
3. H1 Collab., S. Tapprogge, Diffractive Deep-Inelastic Scattering, 1996. To be published in the proceedings of the XXXIe Recontres de Moriond, QCD and High Energy Hadronic Interactions, Les Arcs.
4. ZEUS Collab., M. Derrick et al., Z. Phys. **C 68** (1995) 569
5. ZEUS Collab., M. Derrick et al., Z. Phys. **C 70** (1996) 391
6. ZEUS Collab., Measurement of the Cross Section and t Distribution in Diffractive DIS Events with Leading Protons at HERA, 1996. To be published in the proceedings of the XVIII International Conference on High Energy Physics, Warsaw.
7. E665 Collab., M.R. Adams et al., Phys. Rev. Lett. **75** (1995) 1466
8. E665 Collab., M.R. Adams et al., Z. Phys. **C 67** (1995) 403
9. NMC Collab., P. Amaudruz et al., Nucl. Phys. **B 441** (1995) 3; A. Arneodo et al., Nucl. Phys. **B 441** (1995) 12
10. M. Arneodo et al., Nuclear Beams in HERA, 1996. To be published in the proceedings of the Workshop on Future Physics at HERA (DESY), Hamburg.
11. T.H. Bauer et al., Rev. Mod. Phys. **50** (1978) 261
12. G. Niesler, G. Piller and W. Weise, Phys. Lett. **B 389** (1996) 157
13. ZEUS Collab., M. Derrick et al., Z. Phys. **C 73** (1996) 73
14. ZEUS Collab., M. Derrick et al., Phys. Lett. **B 377** (1996) 259
15. ZEUS Collab., M. Derrick et al., Z. Phys. **C 69** (1995) 39
16. F. Klingl, N. Kaiser and W. Weise, Z. Phys. **A 356** (1996) 193
17. A. Donnachie and P.V. Landshoff, Phys. Lett. **B 296** (1992) 227
18. K. Goulianos, Phys. Rep. **101** (1983) 169
19. A. Donnachie and P.V. Landshoff, Nucl. Phys. **B 244** (1984) 322; Nucl. Phys. **B 267** (1986) 690; Phys. Lett. **B 191** (1987) 309; Phys. Lett. **B 198** (1987) 590; G. Ingelman and P. Schlein, Phys. Lett. **B 152** (1985) 256; E.L. Berger et al., Nucl. Phys. **B 286** (1987) 704; A. Capella et al., Phys. Lett. **B 343** (1995) 403; K. Golec-Biernat and J. Kwiecinski, Phys. Lett. **B 353** (1995) 329; T. Gehrmann and W.J. Stirling, Z. Phys. **C 70** (1996) 89
20. A. Donnachie and P.V. Landshoff, Nucl. Phys. **B 303** (1988) 634
21. P.V. Murthy et al., Nucl. Phys. **B 92** (1975) 269; L.G. Dakhno, Yad. Fiz. **37** (1983) 993
22. L. Bertocchi, Nuovo Cim. **11A** (1972) 45; J.H. Weis, Acta Physica Polonica **B 7** (1976) 851
23. V.N. Gribov, Sov. Phys. JETP **29** (1969) 483
24. M. Lacombe, B. Loiseau, J.M. Richard and R.V. Mau, Phys. Rev. **C 21** (1980) 861
25. B. Badelek and J. Kwiecinski, Nucl. Phys. **B 370** (1992) 278
26. W. Melnitchouk and A. W. Thomas, Phys. Lett. **B 317** (1993) 437
27. G. Piller, W. Ratzka and W. Weise, Z. Phys. **A 352** (1995) 427
28. L.L. Frankfurt and M.I. Strikman, Nucl. Phys. **B 316** (1989) 340
29. N.N. Nikolaev and B.G. Zakharov, Z. Phys. **C 49** (1991) 607; N.N. Nikolaev and V.R. Zoller, Z. Phys. **C 56** (1992) 623
30. D.O. Caldwell et al., Phys. Rev. Lett. **40** (1978) 1222
31. H1, Collab., S. Aid et al., Nucl. Phys. **B 470** (1996) 3, ZEUS Collab., M. Derrick et al., Z. Phys. **C 72** (1996) 399
32. H.L. Lai et al., Phys. Ref. **D 51** (1994) 4763
33. B. Kopeliovich and B. Povh, Z. Phys. **A 356** (1997) 467
34. H1, Collab., S. Aid et al., Nucl. Phys. **B 468** (1996) 3
35. N. Cartiglia, representing the Hl and ZEUS Collab., Diffraction at HERA, 1996. Talk given at the 24th Annual SLAC Summer Institute on Particle Physics, Stanford, preprint hep-ph/9703245